Mirco Cosottini, MD
Marco Giannelli, PhD
Gabriele Siciliano, MD
Guido Lazzarotti, MD
Maria Chiara Michelassi, MD
Alberto Del Corona, MD
Carlo Bartolozzi, MD
Luigi Murri, MD

Published online
10.1148/radiol.2371041506
Radiology 2005; 237:258–264

Abbreviations:
ALS = amyotrophic lateral sclerosis
ALSFRS = ALS Functional Rating Scale
FA = fractional anisotropy
MD = mean diffusivity
PMA = progressive muscular atrophy
ROI = region of interest

[1] From the Departments of Neuroscience (M.C., G.S., A.D.C., L.M.) and Radiology (G.L., M.C.M., C.B.), University of Pisa, via Roma 67, 56100 Pisa, Italy; and Units of Neuroradiology (M.C.) and Medical Physics (M.G.), S. Chiara Hospital, Pisa, Italy. From the 2004 RSNA Annual Meeting. Received August 31, 2004; revision requested November 5; revision received December 3; accepted January 17, 2005. **Address correspondence to** M.C. (e-mail: *mircocosottini@libero.it*).

Authors stated no financial relationship to disclose.

Author contributions:
Guarantors of integrity of entire study, C.B., L.M.; study concepts/study design or data acquisition or data analysis/interpretation, all authors; manuscript drafting or manuscript revision for important intellectual content, all authors; approval of final version of submitted manuscript, all authors; literature research, G.L., M.C.M.; clinical studies, G.S., A.D.C.; statistical analysis, M.G.; and manuscript editing, M.C., M.G., G.S.

Diffusion-Tensor MR Imaging of Corticospinal Tract in Amyotrophic Lateral Sclerosis and Progressive Muscular Atrophy[1]

PURPOSE: To prospectively evaluate several diffusion-tensor magnetic resonance (MR) imaging indexes (mean diffusivity [MD], fractional anisotropy [FA], and eigenvalues) of corticospinal tract impairment in patients with progressive muscular atrophy (PMA) and patients with amyotrophic lateral sclerosis (ALS).

MATERIALS AND METHODS: This study had institutional review board approval, and written informed consent was obtained from all subjects. Eight male patients with PMA (mean age, 63 years ± 13 [standard deviation]), eighteen patients with ALS (14 men and four women; mean age, 64 years ± 7), and twelve control subjects (four men and eight women; mean age, 65 years ± 6) underwent diffusion-tensor MR imaging at which 25 spin-echo echo-planar imaging diffusion-weighted images (b = 1000 sec/mm^2) were acquired along noncollinear directions. MD and FA were measured along the corticospinal tracts in each patient and subject. Changes in diffusion along and orthogonal to fiber bundles in patients were evaluated by using diffusion-tensor eigenvalues. Differences in diffusion-tensor imaging indexes between patients with PMA and those with ALS, as compared with these indexes in control subjects, were evaluated with Mann-Whitney testing. Correlations between diffusion-tensor imaging indexes and clinical variables were estimated with Pearson and Spearman rank correlation testing.

RESULTS: As compared with MD (697.1×10^{-6} mm^2/sec ± 28.1) and FA (0.585 ± 0.032) in control subjects, MD was typically significantly increased (734.7×10^{-6} mm^2/sec ± 41.2, P = .035) and FA significantly decreased (0.534 ± 0.053, P = .037) along the corticospinal tracts in patients with ALS, while these parameters showed no significant change in patients with PMA (MD, 707.0×10^{-6} mm^2/sec ± 44.2; FA, 0.559 ± 0.028). Estimation of diffusion-tensor eigenvalues revealed normal diffusion along fiber tracts in all patients, while diffusion was increased orthogonal to fiber tracts only in patients with typical ALS. In patients with ALS, MD correlated with disease duration while FA correlated with disease severity.

CONCLUSION: Diffusion-tensor MR imaging reveals corticospinal tract impairment in ALS but not in PMA.

Amyotrophic lateral sclerosis (ALS), or Charcot disease, is a progressive neurodegenerative disorder that affects the corticospinal tracts and lower motor neurons and has an incidence rate of 1.2–1.8 per 100 000 individuals (1). Such clinical manifestations of the disease as weakness of voluntary muscles, muscle atrophy, tendon jerks, fasciculations, spasticity, and the Babinski sign are variously present depending on the prevalent involvement of the upper motor neurons or the lower motor neurons. Although signs of upper or lower motor neuron involvement may predominate at disease onset, signs of both upper and lower motor neuron involvement will be present further along in the course of the disease.

Progressive muscular atrophy (PMA) is a rare form of motor neuron disease characterized by weakness and wasting of muscles of the limbs or trunk without evidence of upper motor neuron dysfunction (2). Its nosologic importance with respect to typical ALS is uncertain, and whether and when signs of upper motor neuron involvement will develop further along in the course of PMA cannot be predicted. However, the correct detection of cases of PMA can be worthwhile because disease progression is usually slower and the prognosis more benign with PMA than with typical ALS. Although the lower motor neurons can easily be investigated with electromyography (3), the ascertainment of marked upper motor neuron dysfunction is not easy with current diagnostic tools and often rests strictly on clinical findings.

Neuroimaging is used in ALS to rule out other diagnostic possibilities but does not contribute to enhancing the likelihood of the diagnosis (4). Brain magnetic resonance (MR) imaging has limited value in the diagnostic workup of ALS (5) because of its low sensitivity in the detection of corticospinal tract degeneration, although changes in signal intensity along the internal capsule or primary motor cortex have been observed with use of various MR imaging sequences (6–9). MR spectroscopy has been shown to reveal a reduced concentration of the neuronal marker metabolite *N*-acetylaspartate in the motor cortex of patients with ALS. Nevertheless, spectroscopic methods need to be better standardized for routine clinical evaluation of patients with ALS (10), especially given the advent of absolute metabolite quantification and high-field-strength MR spectroscopic techniques that may overcome some previous limitations of MR spectroscopy (eg, low sensitivity in the early stages of the disease [11,12] and low specificity).

Diffusion-tensor imaging is an MR imaging technique that is sensitized to the diffusive properties of water molecules (13) and offers the possibility of detecting brain injuries earlier than they can be detected with conventional imaging methods (14). Potential clinical applications of diffusion-tensor MR imaging arise from the principle that, during their random diffusion-driven displacements, water molecules probe tissue structures at a microscopic scale that is well beyond the usual image resolution (15). Water diffusion, a three-dimensional process that is not the same in all directions in an anisotropic tissue like brain white matter (16), is fully expressed by means of the effective symmetric diffusion tensor **D** (17).

Diffusion-tensor imaging involves the MR measurement of the diffusion tensor *D* and the analysis and display of the information that it contains (18). Diffusion-tensor imaging enables the measurement of the magnitude and directionality of water diffusion. Diffusion-tensor diagonalization yields eigenvectors and eigenvalues (λ_1, λ_2, and λ_3) that represent the main diffusion directions and associated diffusivities of water molecules (19). In white-matter fibers, the eigenvector associated with the largest eigenvalue (λ_1) indicates the direction of the fastest diffusion that corresponds to the fiber direction. Conversely, the smallest (λ_3) and the middle (λ_2) eigenvalues can be used to estimate the diffusion along the orthogonal directions perpendicular to fiber bundles. Two scalar measures, mean diffusivity (MD) and fractional anisotropy (FA), can be extracted from the diffusion tensor and used to create quantitative maps of isotropic and anisotropic diffusion in tissues, respectively. MD and FA are rotationally invariant diffusion indexes (20) that can be easily compared between individuals because they are orientation independent.

Relatively recently, diffusion-tensor imaging has been applied to the evaluation of corticospinal tract impairment in patients with ALS, in whom a significant increase in MD and reduction in FA have been found (21). Use of this technique in patients with ALS can be justified on the assumption that the degree of orientational coherence of fibers influences water diffusion, and, therefore, changes in the architecture of corticospinal tracts that occur in a neurodegenerative disease such as ALS may affect diffusion-tensor imaging indexes.

On the basis of this background, the aim of our work was to prospectively evaluate several diffusion-tensor imaging indexes (MD, FA, and eigenvalues) of corticospinal tract impairment in patients with PMA and patients with ALS.

MATERIALS AND METHODS

Patients and Control Subjects

Written informed consent was obtained from all participants in this study, and the study was approved by the institutional review board of the University of Pisa. Between July 2003 and January 2004, we examined a total of 26 consecutive patients (22 men and four women) with motor neuron disease that was diagnosed according to the revised El Escorial diagnostic criteria for ALS (22). Eight male patients had a diagnosis of sporadic PMA characterized by asymmetrical distal muscle weakness, wasting, flaccidity, fasciculations, and deep tendon areflexia without corticospinal tract involvement for more than 2 years after the onset of symptoms. Sparing of central motor pathways was confirmed with magnetic transcranial motor evoked potential analysis. Results of genetic analysis for both androgen receptor genes (Kennedy disease) and survival motor neuron genes (spinal muscular atrophy) were negative.

Eighteen patients (14 men and four women) had definite ALS with upper and lower motor neuron involvement that was characterized by distal asymmetric weakness, spasticity, hyperreflexia, loss of dexterity associated with muscle atrophy, and fasciculations. Upper motor neuron involvement was confirmed at electrophysiologic examination with motor evoked potentials that revealed a central motor conduction velocity (mean value, 19.8 msec ± 2.2 [standard deviation] for lower limbs and 9.4 msec ± 3 for upper limbs) that was increased with respect to normal values.

No patient had a family history of ALS, and all patients had negative results at genetic analysis for the Cu/Zn SOD-1 gene mutation. In 16 patients, the onset of symptoms had involved the lower limbs, and in 10 patients it had involved the upper limbs. No bulbar onset or involvement was present in our study group. Clinical evaluation of disease severity was performed by using the ALS Functional Rating Scale (ALSFRS) (23). The ALSFRS scores were not significantly different ($P > .05$) between patients with PMA (30.5 ± 9.1) and patients with ALS (34.7 ± 2.9). The disease duration in patients with PMA was longer (46.25 months ± 10), but not significantly so ($P > .05$), compared with the duration in patients with ALS (33.4 months ± 20). No patient had undergone percutaneous endoscopic gastrostomy, and only one patient with ALS had received noninvasive ventilation.

Twelve volunteer control subjects (four men and eight women) of a mean age (65 years ± 6) that was comparable to the mean ages of the patients with PMA (63 years ± 13, $P > .05$) and the patients with ALS (64 years ± 7, $P > .05$) were also enrolled in the study so that we could avoid a potential age-related bias in terms of tensor indexes (24,25). Control subjects were recruited among nurses of the

Department of Radiology of the University of Pisa and their parents. The control subjects had no history of and negative physical examination results for neurologic disorders and gave informed consent after the aims of the study were explained.

MR and Diffusion-Tensor Imaging

Examinations were performed with 1.5-T MR imaging equipment (Signa Infinity Twinspeed; GE Medical Systems, Milwaukee, Wis) with a maximum gradient strength of 40 mT/m and a slew rate of 150 $(T \cdot m^{-1})$/sec. A standard quadrature head coil was used for radiofrequency transmission and reception of the MR signal. The MR imaging protocol included a fluid-attenuated inversion recovery sequence in the transverse plane that covered the brain along the bicommissural axis (repetition time msec/echo time msec/inversion time msec, 8000/90/2000; field of view, 24 × 24 cm; section thickness, 5 mm; intersection gap, 1 mm; matrix, 224 × 224; number of signals acquired, one). Images obtained with the conventional sequence were evaluated by a single radiologist (M.C., who had 13 years of experience in interpreting brain MR images) who was blinded to the clinical status of the patient. This radiologist assessed the presence or absence of areas of hyperintense signal in the corticospinal tracts.

The diffusion tensor **D** is generally estimated after at least six diffusion-weighted images along noncollinear directions and a reference image without diffusion weighting are acquired. In our study, diffusion-weighted images were obtained with a spin-echo echo-planar imaging sequence (26) (repetition time msec/echo time msec, 6500/79.9; field of view, 24 × 24 cm; section thickness, 5 mm; intersection gap, 1 mm; matrix, 128 × 128; number of signals acquired, two; acquisition time, 5 minutes 51 seconds) that was sensitized to water diffusion by means of a strong magnetic field gradient pulse (b = 1000 sec/mm^2) (27). We decided to use a diffusion-weighted imaging scheme that involved 25 diffusion-encoding gradient directions for sampling space more uniformly, reducing noise, and improving the precision of diffusion-tensor imaging measurements (28).

The signal attenuation due to diffusion and the field gradient pulse applied is expressed by the following equation:

$$\ln[S_b/S_{b=0}] = -\sum_{i,j=1}^{3} b_{ij}\mathbf{D}_{ij}, \qquad (1)$$

where S_b and $S_{b=0}$ are the signal intensities on the diffusion-weighted image and the reference image, respectively; $\mathbf{D}_{ij}$ represents the elements of the diffusion tensor; and b_{ij} represents the components of the symmetric b matrix b (29). The six independent elements ($\mathbf{D}_{ij}$) of the diffusion tensor were estimated voxelwise by performing multivariant linear least-square fitting of Equation (1). Diffusion-tensor diagonalization yields eigenvectors and eigenvalues (λ_1 is the largest eigenvalue, λ_2 is the middle eigenvalue, and λ_3 is the smallest eigenvalue) that represent the main orthogonal diffusion directions and the associated diffusivities of every voxel (19).

Maps of the rotationally invariant indexes MD and FA were calculated. MD describes the magnitude of diffusivity regardless of direction, and use of this index removes the effects of directionality from diffusion measurements in anisotropic media. The MD was estimated from the sum of the diffusion-tensor eigenvalues as follows:

$$\mathrm{MD} = \tfrac{1}{3}(\lambda_1 + \lambda_2 + \lambda_3). \qquad (2)$$

FA is a dimensionless index that reflects the degree of anisotropy in tissues. It was estimated from the fraction of the magnitude of the diffusion tensor related to anisotropy by using the following equation:

$$\mathrm{FA} = \sqrt{(3/2)} \cdot \sqrt{(\lambda_1 - \mathrm{MD})^2 + (\lambda_2 - \mathrm{MD})^2 + (\lambda_3 - \mathrm{MD})^2}/\sqrt{(\lambda_1^2 + \lambda_2^2 + \lambda_3^2)}. \qquad (3)$$

FA values range from 0 (for an isotropic medium) to 1 (for a medium with the highest degree of anisotropy).

The MD and FA and the largest (λ_1), smallest (λ_3), and middle (λ_2) eigenvalues were measured along the corticospinal tracts visualized on the FA maps. Two regions of interest (ROIs) of 26 mm^2 each—one in the posterior limb of the internal capsule and one in the middle part of the cerebral peduncles on both sides—were placed by a single operator (G.L., who had 4 years of experience in interpreting brain MR images), and two other ROIs of 26 mm^2 and 11 mm^2, respectively, were traced in the pons and in the pyramids of the medulla on both sides. Altogether, we placed 10 ROIs along both corticospinal tracts for each patient (Fig 1). MD, FA, λ_1, λ_2, and λ_3 were measured for each ROI location level so that we could evaluate the distribution of diffusion-tensor imaging parameters along the corticospinal tract in control subjects and in patients. Fiber tract asymmetry was assessed by comparing mean MD, FA, λ_1, λ_2, and λ_3 along the right and the left corticospinal tracts in patients with PMA, patients with ALS, and control subjects. Finally, the values of each diffusion-tensor imaging index in the 10 ROIs were averaged to obtain a single mean diffusion-tensor imaging parameter (FA, MD, λ_1, λ_2, and λ_3) along the corticospinal tracts for each patient and control subject.

Statistical Analysis

Asymmetries in mean MD, FA, and eigenvalue measurements between the right and the left corticospinal tracts of patients and control subjects were evaluated with the two-tailed Wilcoxon test for paired samples. After a preliminary power analysis, differences in diffusion-tensor imaging parameters between the patients with PMA and the patients with ALS with respect to these parameters in the control subjects were assessed with a nonparametric two-tailed Mann-Whitney test and Bonferroni correction for multiple comparisons. On the basis of results of previous work (21), power calculation was performed given the assumption of minimum detectable mean differences of 50×10^{-6} mm^2/sec ± 30 for the single mean MD, λ_1, λ_2, and λ_3 values and 0.04 ± 0.03 for the single mean FA value, with $\alpha < .05$ (type I error) corrected for multiple comparisons. The threshold of statistical significance was set at $P \leq .05$. Correlations between clinical variables (disease duration and ALSFRS score) and single mean FA, MD, λ_1, λ_2, and λ_3 values were investigated with Pearson and Spearman rank correlation testing, respectively. Statistical analyses were performed by using SPSS, version 10.1.0 (SPSS, Chicago, Ill) and GPower, version 2.0 (F. Faul and E. Erdfelder, Bonn University; available at *http://www.psycho.uni-duesseldorf.de/aap/projects/gpower*).

RESULTS

MR Imaging

On fluid-attenuated inversion recovery images, hyperintense signal in the posterior limb of the internal capsule was detected in only two patients with ALS.

MD, FA, and Eigenvalues

No side-related significant difference in mean MD, FA, λ_1, λ_2, or λ_3 values in the five ROIs along both corticospinal tracts was observed in patients with PMA, patients with ALS, or control subjects.

The MD had a tendency to increase and FA had a tendency to decrease from the internal capsule to the pyramids in both patients and control subjects. In Figure 2, the MD and FA measured at different levels of the corticospinal tract in the control group are reported.

Results of statistical analysis indicated a high power for all comparisons between patients and control subjects, except for the comparison of single mean FA value between patients with PMA and control subjects, for which there was medium power. The single mean MD value in patients with ALS, but not that in patients with PMA, was significantly increased ($P = .035$) compared with that in the control group. Similarly, the single mean FA value in patients with ALS, but not that in patients with PMA, was significantly decreased ($P = .037$) compared with that in the control group. The single mean largest eigenvalue (λ_1) in both the patients with PMA and the patients with ALS was not significantly different from that in the control group. Both the single mean middle (λ_2) and smallest (λ_3) eigenvalues in the patients with ALS, but not those in the patients with PMA, were significantly increased ($P = .024$ for λ_2, $P = .017$ for λ_3) with respect to these eigenvalues in the control group. The single mean MD, FA, λ_1, λ_2, and λ_3 values in the patients with PMA, the patients with ALS, and the control group are reported in Table 1.

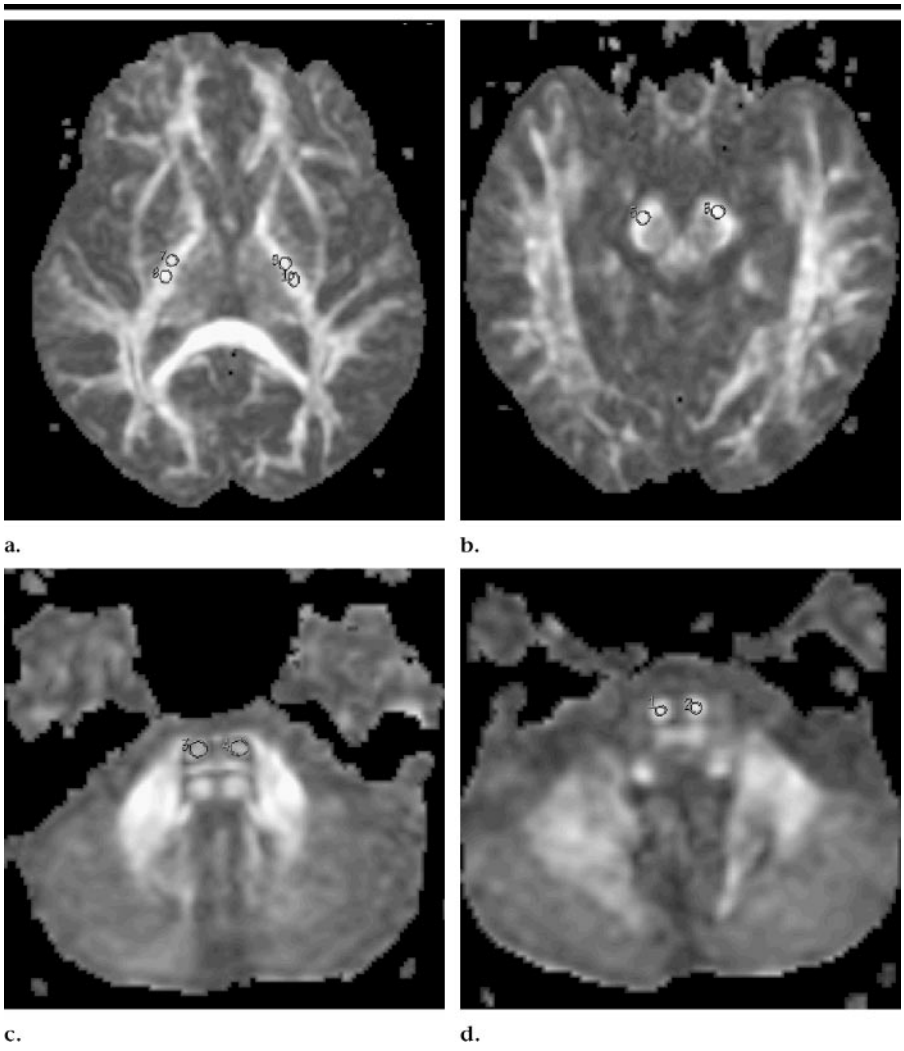

Figure 1. FA maps acquired at different levels along corticospinal tracts. FA maps were calculated after the acquisition of 25 spin-echo echo-planar imaging diffusion-weighted MR images (6500/79.9; field of view, 24 × 24 cm; section thickness, 5 mm; intersection gap, 1 mm; matrix, 128 × 128; number of signals acquired, two; $b = 1000$ sec/mm^2) along noncollinear directions and a reference image without diffusion weighting. For each patient and control subject, two ROIs were placed in **(a)** both internal capsules, and one ROI was placed on both sides of the **(b)** cerebral peduncles, **(c)** pons, and **(d)** pyramids. Single mean FA, MD, λ_1, λ_2, and λ_3 values were estimated from the averaged values of the diffusion-tensor imaging parameters in the 10 ROIs.

Correlation between Diffusion-Tensor Imaging Indexes and Clinical Variables

The single mean MD, FA, λ_1, λ_2, and λ_3 values in the patients with PMA did not correlate with either disease duration or ALSFRS score. In the patients with ALS, the single mean FA, λ_3, and λ_2 values did not correlate with disease duration, while MD and λ_1 did; in addition, MD, λ_1, and λ_2 did not correlate with ALSFRS score, while FA and λ_3 did. The coefficients of correlation between diffusion-tensor imaging indexes and clinical variables are reported in Table 2.

DISCUSSION

Fluid-attenuated inversion recovery sequences are widely used as one of the more reliable MR imaging acquisition techniques for assessing the presence of areas of hyperintense signal in the corticospinal tracts of patients with ALS (8). In our study, fluid-attenuated inversion recovery MR images revealed areas of hyperintense signal in the internal capsule as a marker of a degenerative process of the upper motor neurons in only two patients with ALS, indicating that conventional MR imaging is not a suitable diagnostic tool for corticospinal tract investigation in ALS (30).

Despite previous observations about FA asymmetry in the internal capsule that is not associated with handedness (31), we did not find significant differences in diffusion parameters between right and left sides. Moreover, our results confirm the downward trend in FA and upward trend in MD from the internal capsule to the pyramids along the corticospinal tract (31). This was why we preferred to average the diffusion-tensor imaging values of all the ROIs measured along the corticospinal tracts to obtain a single index value representative of the entire corticospinal tracts. This strategy also permits one to reduce the weight of a possible confounding bias in diffusion-tensor imaging measurements in some regions like the rostral pons, where a modification of FA or MD can be related not only to fiber loss but also to the cross-

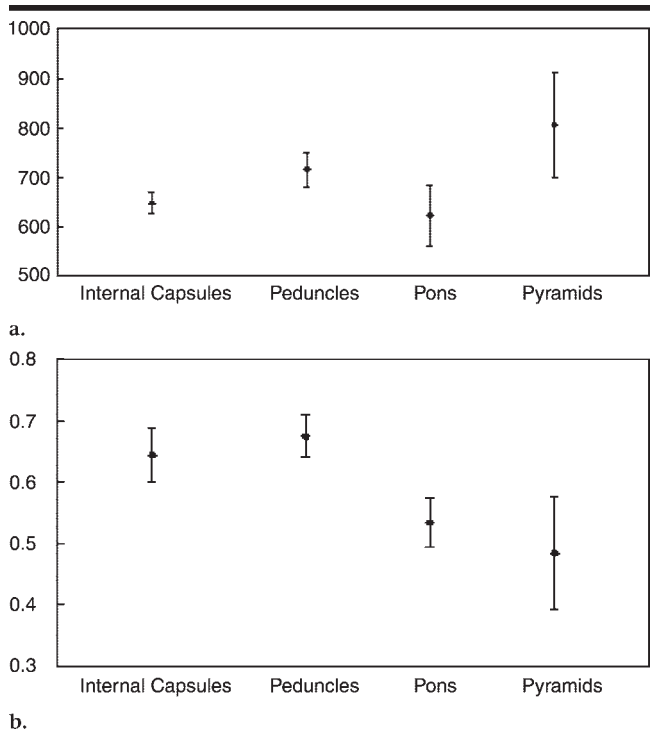

Figure 2. Graphs show **(a)** MD ($\times 10^{-6}$ mm^2/sec) and **(b)** FA (dimensionless) at different levels of the corticospinal tract in control subjects. The data points indicate mean values, and the error bars indicate standard deviations.

TABLE 1
Diffusion-Tensor Imaging Indexes in Patients with PMA or ALS versus Those in Control Subjects

Diffusion-Tensor Imaging Index	Patients with PMA	Patients with ALS	Control Subjects
MD ($\times 10^{-6}$ mm^2/sec)	707.0 ± 44.2	734.7 ± 41.2*	697.1 ± 28.1
FA	0.559 ± 0.028	0.534 ± 0.053†	0.585 ± 0.032
λ_1 ($\times 10^{-6}$ mm^2/sec)	1219.2 ± 61.8	1216.8 ± 71	1222.4 ± 60.4
λ_2 ($\times 10^{-6}$ mm^2/sec)	543.1 ± 47.8	583.5 ± 58*	522.9 ± 38.1
λ_3 ($\times 10^{-6}$ mm^2/sec)	368.2 ± 47.2	395.4 ± 46.7*	347.2 ± 35.7

Note.—Data are single mean values averaged across 10 ROIs ± standard deviations.
* Significantly increased compared with the value in control subjects ($P = .035$).
† Significantly decreased compared with the value in control subjects ($P = .037$).

ings between the corticospinal tract and transverse pontine fibers (32,33).

Our diffusion-tensor imaging results revealed a significant reduction in FA and increase in MD along the corticospinal tract in patients with ALS. The augmentation of MD, a measure of water diffusivity, may represent the expression of extracellular volume increase secondary to axonal loss and fiber density reduction, findings consistent with what has been reported in other conditions characterized by tissue rarefaction, such as multiple sclerosis (34,35) and chronic ischemia (36,37). In line with this interpretation, MD showed a positive correlation with disease duration, a finding that is probably related to the pathologic effects of the underlying disease process that result in neuronal loss in patients with ALS. On the other hand, we believe that the reduction in FA reflects a different pathologic effect because it showed a correlation with disease severity but not with disease duration in patients with ALS. This observation has previously been reported in a study of ALS with bulbar onset (21) but was not confirmed in another study (31).

To obtain further insight into the structural changes of the corticospinal tracts in ALS, we evaluated the behavior of the eigenvalues that determine the observed MD and FA changes. There is evidence that in ALS the neurodegenerative process is not exclusive to the motor pathways but also affects the basal ganglia, the limbic system, and the intermediate zone of the spinal cord (38). Because relevant detectable decreases in anisotropy arise only from structural modifications in regions with normally high anisotropy (39), we calculated the eigenvalues, as well as MD and FA, exclusively along the corticospinal tracts, which have high anisotropy owing to their highly ordered white matter content. On the basis of our eigenvalues data, it can be argued that the decreased anisotropy we observed in patients with ALS arose from increased diffusion transverse to nerve fibers (as indicated by the increased λ_2 and λ_3 values) rather than decreased diffusion along the fiber bundles (as indicated by the unchanged λ_1 value). Therefore, in the corticospinal tract, patients with ALS may have a reduction in FA combined with an increase in MD owing to increased diffusivity only orthogonal to the fibers. This diffusion-tensor imaging parameter profile is considered a signature of wallerian degeneration (33) that represents secondary white matter degeneration.

In primary lesions in which the fiber loss results from direct white matter injury, as in stroke (33) or the acute plaques of multiple sclerosis (40), the diffusion impairment includes a consistent augmentation of isotropic diffusion (ie, of MD) and an increased diffusivity parallel to the fibers (λ_1), while in wallerian degeneration, MD is less impaired and λ_1 is not increased. Such interpretations ensue from similar results observed in animal models of wallerian degeneration that revealed a reduction in diffusion anisotropy with decreased (41) or unchanged (42) diffusivity in the direction parallel to the fibers. In these pathologic and MR imaging correlative studies, ultrastructural or histologic examination revealed demyelination, inflammation, and axonal loss. The augmented extracellular space with gliosis promotes the diffusion of water molecules orthogonal to the fibers' axis while limiting the diffusion along the fiber tracts.

Taking into account the fact that the main histologic finding of degeneration along the corticospinal tracts in ALS is loss of motor neurons and astrocytosis (43–45) with depletion of large myelinated fibers (46), our diffusion-tensor imaging results seem to be occasioned by similar histologic changes (47) consistent

with the occurrence of wallerian degeneration in corticospinal tracts. In particular, the axonal loss and collapse of myelin destroys the distinction between the intra- and the extra-axonal water environment, thereby removing obstacles to orthogonal diffusion. Furthermore, macrophage infiltration of corticospinal tracts (48) may cause increased obstruction of longitudinal diffusion. This pattern of altered diffusivity cannot be considered specific for ALS because similar results have been observed in the apparently normal white matter of patients with relapsing-remitting multiple sclerosis (39); instead, it could be considered indicative of histologic changes secondary to white matter degeneration of different origin.

Our diffusion-tensor imaging results in patients with PMA (a pure lower motor neuron disease) are consistent with pathologic findings that have been reported for PMA. Neuronal loss and gliosis in the anterior horn of the spinal cord and the motor nuclei of the brainstem and the absence of corticospinal tract lesions have been considered the only definite diagnostic criteria for PMA (49).

Recently, diffusion-tensor imaging has been shown to be able to reveal early upper motor neuron involvement in patients with ALS and lower motor neuron impairment before clinical symptoms of corticospinal tract lesions become apparent (50). In indicating that diffusion-tensor imaging abnormalities do not occur in patients with PMA, our results could suggest the conclusion that patients with solely lower motor neuron involvement of long duration can be given a diagnosis of PMA.

However, PMA has been considered to be a distinct nosologic entity from typical ALS (51) owing to its slow progression, indolent course (1), and long duration with high survival rate (52). To date, considering PMA as a separate disease has been controversial and sometimes rejected, given that corticospinal system involvement can occur at a certain time in the disease course. In line with this, some reports have indicated that there is myelin pallor along the corticospinal tracts in a proportion of patients with PMA (53–55)—even patients with long disease duration (56,57)—suggesting that at least some patients with clinically diagnosed PMA have a subtype of ALS.

It has recently been reported that use of CD68, a macrophage activation marker, at immunohistochemistry can reveal pathologic corticospinal tract abnormalities in 50% of patients with PMA, whereas use of Luxol fast blue or Marchi staining reveals such abnormalities in only 20% of patients (58). On the basis of these findings, we cannot exclude the possibility that some patients with PMA could have an impairment of the long spinal tracts that is clinically undetectable because of profound terminal amyotrophy. Anyway, if this is the case, diffusion-tensor imaging would not be able to reveal (as well as conventional myelin stains could) corticospinal tract involvement in patients with PMA.

The main limitation of this study was the fact that we evaluated the corticospinal tract exclusively in the internal capsule and brainstem, where the pathologic hallmarks of ALS are less conspicuous with respect to these hallmarks in the spinal cord. Nevertheless, to date, diffusion-tensor imaging of the spinal cord remains a challenge because it is limited by the susceptibility artifacts generated in and the small dimensions of this anatomic region (59).

In conclusion, such diffusion-tensor imaging parameters as MD and FA obtained along the corticospinal tracts enable the differentiation of patients with ALS from control subjects. The modifications in the diffusion-tensor eigenvalues observed in this study indicate that the underlying structural changes in ALS could be caused by nerve tract degeneration of the secondary fibers that resembles wallerian degeneration. In addition, diffusion-tensor imaging did not reveal any corticospinal tract abnormality in patients with PMA.

TABLE 2
Correlations between Diffusion-Tensor Imaging Indexes and Clinical Variables

Clinical Variable and Diffusion-Tensor Imaging Index*	Patients with PMA		Patients with ALS	
	r Value	*P* Value	*r* Value	*P* Value
Disease duration				
MD ($\times 10^{-6}$ mm^2/sec)	−0.261	>.05	0.659	.0029
FA	0.389	>.05	0.160	>.05
λ_1 ($\times 10^{-6}$ mm^2/sec)	−0.417	>.05	0.760	.0003
λ_2 ($\times 10^{-6}$ mm^2/sec)	−0.379	>.05	0.377	>.05
λ_3 ($\times 10^{-6}$ mm^2/sec)	−0.228	>.05	0.189	>.05
ALSFRS score				
MD ($\times 10^{-6}$ mm^2/sec)	0.390	>.05	−0.302	>.05
FA	−0.683	>.05	0.639	.004
λ_1 ($\times 10^{-6}$ mm^2/sec)	0.634	>.05	0.462	>.05
λ_2 ($\times 10^{-6}$ mm^2/sec)	0.585	>.05	−0.412	>.05
λ_3 ($\times 10^{-6}$ mm^2/sec)	0.393	>.05	−0.562	.015

* Diffusion-tensor imaging indexes as averaged across 10 corticospinal tract ROIs.

Acknowledgment: We thank Lorenzo Faggioni, MD, for statistical analysis.

References

1. Strong M. Rosenfeld J. Amyotrophic lateral sclerosis: a review of the current concepts. Amyotroph Lateral Scler Other Motor Neuron Disord 2003;4:136–143.
2. Swash M. Clinical features and diagnosis of amyotrophic lateral sclerosis. In: Brown R, Meininger V, Swash M, eds. Amyoptrophic lateral sclerosis. London, England: Dunitz, 2000.
3. de Carvalho M, Johnsen B, Fuglsang-Frederiksen A. Medical technology assessment: electrodiagnosis in motor neuron diseases and amyotrophic lateral sclerosis. Neurophysiol Clin 2001;31:341–348.
4. Brooks BR. El Escorial World Federation of Neurology Criteria for the diagnosis of amyotrophic lateral sclerosis. J Neurol Sci 1994;124(suppl):96–107.
5. Chan S, Kaufmann P, Shungu DC, Mitsumoto H. Amyotrophic lateral sclerosis and primary lateral sclerosis: evidence-based diagnostic evaluation of the upper motor neuron. Neuroimaging Clin N Am 2003;13:307–326.
6. Hofmann E, Ochs G, Pelzl A, Warmuth-Metz M. The corticospinal tract in amyotrophic lateral scerosis: an MRI study. Neuroradiology 1998;40:71–75.
7. Cheung G, Gawel MJ, Cooper PW, et al. Amyotrophic lateral sclerosis: correlation of clinical and MRI findings. Radiology 1995;194:263–270.
8. Hecht MJ, Fellner F, Fellner C, et al. MRI-FLAIR images of the head show corticospinal tract alterations in ALS patients more frequently than T2-, T1- and proton-density-weighted images. J Neurol Sci 2001; 186:37–44.
9. da Rocha AJ, Oliveira AS, Fonseca RB, Maia AC Jr, Buainain RP, Lederman HM. Detection of corticospinal tract compromise in amyotrophic lateral sclerosis with brain MR imaging: relevance of the T1-weighted spin-echo magnetization transfer contrast sequence. AJNR Am J Neuroradiol 2004;25: 1509–1515.
10. Kalra S, Arnold DL. Imaging: MRS, MRI, PET/SPECT—con. Amyotroph Lateral Scler Other Motor Neuron Disord 2002;3(suppl 1):S73–S74.

11. Suhy J, Miller RG, Rule R, et al. Early detection and longitudinal changes in amyotrophic lateral sclerosis by (1)H MRSI. Neurology 2002;58:773–779.
12. Ellis CM, Simmons A, Andrews C, et al. A proton magnetic resonance spectroscopic study in ALS: correlation with clinical findings. Neurology 1998;51:1104–1109.
13. Basser PJ, Mattiello J, Le Bihan D. Estimation of the effective self-diffusion tensor from the NMR spin-echo. J Magn Reson B 1994;103:247–254.
14. Neil J, Miller J, Mukherjee, Huppi S. Diffusion tensor imaging of normal and injured developing human brain: a technical review. NMR Biomed 2002;15:543–552.
15. Le Bihan D, Mangin JF, Poupon C, et al. Diffusion tensor imaging: concepts and applications. J Magn Reson Imaging 2001; 13:534–546.
16. Chenevert TL, Brunberg JA, Piper JG. Anisotropic diffusion within human white matter: demonstration with NMR techniques in vivo. Radiology 1990;177:401–405.
17. Crank J. The mathematics of diffusion. Oxford, England: Clarendon, 1975.
18. Basser PJ, Jones DK. Diffusion-tensor MRI: theory, experimental design and data analysis. NMR Biomed 2002;15:456–467.
19. Basser PJ, Mattiello J, Le Bihan D. MR diffusion tensor spectroscopy and imaging. Biophys J 1994;66:259–267.
20. Pierpaoli C, Basser PJ. Toward a quantitative assessment of diffusion anisotropy. Magn Reson Med 1996;36:893–906.
21. Ellis CM, Simmons A, Jones DK, et al. Diffusion tensor MRI assesses corticospinal tract damage in ASL. Neurology 1999;53: 1051–1058.
22. Brooks BR, Miller RG, Swash M, Munsat TL; World Federation of Neurology Research Group on Motor Neuron Diseases. El Escorial revisited: revised criteria for the diagnosis of amyotrophic lateral sclerosis. Amyotroph Lateral Scler Other Motor Neuron Disord 2000;1:293–299.
23. The ALS CNTF treatment study (ACTS) phase I-II Study Group. The Amyotrophic Lateral Sclerosis Functional Rating Scale: assessment of activities of daily living in patients with amyotrophic lateral sclerosis. Arch Neurol 1996;53:141–147.
24. Gideon P, Thomsen C, Henriksen O. Increased self-diffusion of brain water in normal aging. J Magn Reson Imaging 1994;4: 185–188.
25. Rovaris M, Iannucci G, Cercignani M, et al. Age-related changes in conventional, magnetization transfer, and diffusion-tensor MR imaging findings: study with whole-brain tissue histogram analysis. Radiology 2003;227:731–738.
26. Haacke EM, Brown RW, Thomson MR, Venkatesan R. Magnetic resonance imaging: physical principles and sequence design. New York, NY: Wiley, 1999.
27. Stejskal EO, Tanner JE. Spin diffusion measurements: spin echoes in the presence of a time dependent field gradient. J Chem Phys 1965;42:288–292.
28. Papadakis NG, Xing D, Huang CL, Hall LD, Carpenter TA. A comparative study of acquisition schemes for diffusion tensor imaging using MRI. J Magn Reson 1999;137: 67–82.
29. Mattiello J, Basser PJ, Le Bihan D. Analytical expression for the b matrix in NMR diffusion imaging and spectroscopy. J Magn Reson A 1994;108:131–141.
30. Iwasaki Y, Ikeda K, Ichikawa Y, Igarashi O, Kinoshita M. MRI in ALS patients. Acta Neurol Scand 2003;107:426.
31. Toosy AT, Werring DJ, Orrel RW, et al. Diffusion tensor imaging detects corticospinal tract involvement at multiple levels in amyotrophic lateral sclerosis. J Neurol Neurosurg Psychiatry 2003;74:1250–1257.
32. Tuch D, Weisskoff R, Belliveau J, Wedeen V. High angular resolution diffusion imaging of the human brain sequence (abstr). In: Proceedings of the Seventh Meeting of the International Society for Magnetic Resonance in Medicine. Berkeley, Calif: International Society for Magnetic Resonance in Medicine, 1999; 321.
33. Pierpaoli C, Barnett A, Pajevic S, et al. Water diffusion changes in wallerian degeneration and their dependence on white matter architecture. Neuroimage 2001;13:1174–1185.
34. Werring DJ, Clark CA, Barker GJ, Thompson AJ, Miller DH. Diffusion tensor imaging of lesions and normal appearing white matter in multiple sclerosis. Neurology 1999;52:1626–1632.
35. Cercignani M, Bozzali M, Iannucci G, Comi G, Filippi M. Magnetization transfer ratio and mean diffusivity of normal appearing white and grey matter from patients with multiple sclerosis. J Neurol Neurosurg Psychiatry 2001;70:311–317.
36. Lutsep HL, Albers GW, DeCrespigny A, Kamat GN, Marks MP, Moseley ME. Clinical utility of diffusion-weighted magnetic resonance imaging in the assessment of ischemic stroke. Ann Neurol 1997;41:574–580.
37. Sotak CH. The role of diffusion tensor imaging in the evaluation of ischemic brain injury. NMR Biomed 2002;15:561–569.
38. Ince PG, Lowe J, Shaw PJ. Amyotrophic lateral sclerosis: current issue in classification, pathogenesis and molecular pathology. Neuropathol Appl Neurobiol 1998; 24:104–117.
39. Henry RG, Oh J, Nelson S, Pelletier D. Directional diffusion in relapsing-remitting multiple sclerosis: a possible in vivo signature of wallerian degeneration. J Magn Reson Imaging 2003;18:420–426.
40. Bammer R, Augustin M, Strasser-Fuchs S, et al. Magnetic resonance diffusion tensor imaging for characterizing diffuse and focal abnormalities in multiple sclerosis. Magn Reson Med 2000;44:583–591.
41. Beaulieu C, Does MD, Snyder R. Changes in water diffusion due to wallerian degeneration in peripheral nerve. Magn Reson Med 1996;36:627–631.
42. Stanisz GJ, Midha R, Munro CA, Henkelman RM. MR properties of rat sciatic nerve following trauma. Magn Reson Med 2001; 45:415–420.
43. Greenfield JG, Graham DI, Lantos PL. Greenfield's neuropathology. London, England: Arnold, 1997.
44. Hirano A, Kurland LT, Sayre GP. Familial amyotrophic lateral sclerosis: a subgroup characterized by posterior spinocerebellar involvement and hyaline inclusions in the anterior horn cells. Arch Neurol 1967;16: 232–243.
45. Piao YS, Wakabayashi K, Kakita A, et al. Neuropathology with clinical correlations of sporadic amyotrophic lateral sclerosis: 102 autopsy cases examined between 1962 and 2000. Brain Pathol 2003;13:10–22.
46. Sobue G, Hashizume Y, Mitsuma T, Takanashi A. Size-dependent myelinated fiber loss in the corticospinal tract in Shy-Drager syndrome and amyotrophic lateral sclerosis. Neurology 1987;37:529–532.
47. Dal Canto MC, Gurney ME. Neuropathological changes in two lines of mice carrying a transgene for mutant human Cu,Zn SOD, and in mice overexpressing wild type human SOD: a model of familial amyotrophic lateral sclerosis (FALS). Brain Res 1995;676:25–40.
48. Ince P. Neuropathology. In: Brown R, Meininger V, Swash M, eds. Amyoptrophic lateral sclerosis. London, England: Dunitz, 2000.
49. Bonduelle M. Amyotrophic lateral sclerosis. In: Vinken PJ, Bruyn GW, Klawans HL, Rose FC, eds. Handbook of clinical neurology. Vol 22. System disorders and atrophies. Part II. Amsterdam, the Netherlands: Elsevier, 1975; 281–338.
50. Sach M, Winkler G, Glauche V, et al. Diffusion tensor MRI of early upper motor neuron involvement in amyotrophic lateral sclerosis. Brain 2004;127:340–350.
51. Swank RL, Putnam TJ. Amyotrophic lateral sclerosis and related conditions. Arch Neurol Psychiatry 1943;49:151–177.
52. Chio A, Brignolio F, Leone M, et al. A survival analysis of 155 cases of progressive muscular atrophy. Acta Neurol Scand 1985;72:407–413.
53. Dejerine J, Long E. Examen histologique d'un cas de poliomyelite anterieure cronique. Rev Neurol 1912;1:372–376.
54. Foix C, Chavany JA. Existe-t-il des formes de transition entre la poliomyelite anterieure chronique et la sclerose laterale amyotrophique? Rev Neurol 1925;I:826–827.
55. Brownell B, Oppeheimer DR, Hughes JT. The central nervous system in motor neurone disease. J Neurol Neurosurg Psychiatry 1970;33:338–357.
56. Iwanaga K, Hayashi S, Oyake M, et al. Neuropathology of sporadic amyotrophic lateral sclerosis of long duration. J Neurol Sci 1997;146:139–143.
57. Tsuchiya K, Shintani S, Kikuchi M, et al. Sporadic amyotrophic lateral sclerosis of long duration mimicking spinal progressive muscular atrophy: a clinicopathological study. J Neurol Sci 1999;162:174–178.
58. Ince PG, Evans J, Knopp M, et al. Corticospinal tract degeneration in the progressive muscular atrophy variant of ALS. Neurology 2003;60:1252–1258.
59. Bammer R, Fazekas F. Diffusion imaging of the human spinal cord and the vertebra. Top Magn Reson Imaging 2003;14:461–476.